General scaling laws of chaotic escape in dissipative multistable systems subjected to autoresonant excitations

2010 J. Phys. A: Math. Theor. 43 222002

(http://iopscience.iop.org/1751-8121/43/22/222002)

IOP FTC
IOP PUBLISHING JOURNAL OF PHYSICS A: MATHEMATICAL AND THEORETICAL

J. Phys. A: Math. Theor. **43** (2010) 222002 (8pp) doi:10.1088/1751-8113/43/22/222002

FAST TRACK COMMUNICATION

General scaling laws of chaotic escape in dissipative multistable systems subjected to autoresonant excitations

Ricardo Chacón

Departamento de Física Aplicada, Escuela de Ingenierías Industriales, Universidad de Extremadura, Apartado Postal 382, E-06071 Badajoz, Spain

E-mail: rchacon@unex.es

Received 9 February 2010, in final form 21 April 2010
Published 11 May 2010
Online at stacks.iop.org/JPhysA/43/222002

Abstract

Theory concerning the emergence and control of chaotic escape from a potential well by means of autoresonant excitations is presented in the context of generic, dissipative and multistable systems. General scaling laws relating both the onset and lifetime of transient chaos to the parameters of autoresonant excitations are derived theoretically using vibrational mechanics, Melnikov analysis and energy-based autoresonance theory. Numerical experiments show that these scaling laws are robust against both the presence of noise and driving re-shaping.

PACS numbers: 05.45.Gg, 33.80.Gj

(Some figures in this article are in colour only in the electronic version)

Escape from a potential well is an old problem with wide-ranging implications where the interplay of noise, dissipation, deterministic driving and quantum uncertainty has given rise to unexpected and intriguing phenomena such as coherent destruction of tunneling [1] and stochastic resonance [2]. Other specific examples are pulse-shape-controlled tunneling [3], shot-noise-driven escape in Josephson junctions [4] and thermally induced escape [5]. While most previous investigations on driven escape have restricted themselves to purely periodic drivings, chirped excitations also have a demonstrated effectiveness. Chirped lasers, for example, can reduce the intensity required for infrared multiphoton dissociation of diatomic molecules to an experimentally realizable intensity range [6]. And chirped optical pulses have been shown to enhance charge flow in molecular-tunneling junctions [7]. In spite of the importance of chirped excitations [8], to the best of the author's knowledge, laws governing (some of) the associated escape scenarios remain to be revealed. The key to understanding the aforementioned effectiveness of chirped excitations is essentially the autoresonance (AR) mechanism: AR-induced energy amplification in nonlinear, driven and deterministic systems occurs when the system continuously adjusts its amplitude so that its instantaneous nonlinear period matches the instantaneous driving period of the chirped excitation. Initially studied in

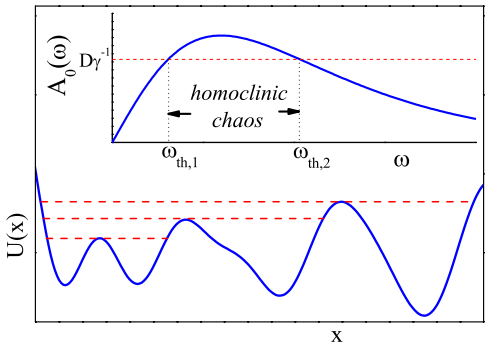

Figure 1. Generic multistable potential $U(x)$ versus x, and energy levels corresponding to different separatrices (dashed lines). The inset shows a generic chaotic threshold function $A_0(\omega)$ versus ω, and the range $[\omega_{\mathrm{th},1}, \omega_{\mathrm{th},2}]$ in which homoclinic chaos is expected (see equation (3)).

the context of a Hamiltonian description, AR phenomena have been well known for about half a century and have been observed in particle accelerators, planetary dynamics, atomic and molecular physics, and nonlinear oscillators [9], to cite a few examples. Regarding dissipative systems, energy-based AR (EBAR) theory has recently been proposed and applied to the case where the system crosses a separatrix associated with its underlying integrable counterpart [10]. Since in such an escape situation the appearance of transient chaos associated with the occurrence of homoclinic bifurcations is a ubiquitous phenomenon, the question naturally arises: How does AR control the chaotic escape scenario, i.e. the onset and lifetime of transient chaos in generic dissipative multistable systems?

In this work, this fundamental problem is studied in the context of the family of systems

$$\ddot{x} + \mathrm{d}U/\mathrm{d}x = -\eta\dot{x} + \gamma \sin[\Omega(t)t], \tag{1}$$

where $U(x)$ is a generic multistable potential (see figure 1) and $\Omega(t) \equiv \omega + \alpha_n t^n$, $n = 1, 2, \ldots$, is a time-dependent frequency with α_n being the nth-order sweep rate. One expects [10] $\gamma \sin[\Omega(t)t]$ to behave as an effective autoresonant excitation whenever the sweep rate is sufficiently low (adiabatic regime), which is the case considered throughout the present communication in order to apply Melnikov analysis (MA) to autoresonant excitations. Note that optimal (exact) AR excitations are generally nonperiodic and unbounded [10], while MA remains valid for nonperiodic temporal perturbations if they are bounded [11]. Also, the damping and autoresonant excitation terms are taken to be small amplitude perturbations of the underlying integrable system so as to deduce analytical expressions for the scaling laws relating both the onset time t_i and lifetime τ of transient chaos to the parameters of the AR excitation from the MA results [12]. The application of MA to any homoclinic (or heteroclinic) orbit $[x_{h,j}(t), \dot{x}_{h,j}(t)]$ of the unperturbed ($\eta = \gamma = 0$) counterpart of equation (1) involves calculating the corresponding Melnikov function (MF):

$$\begin{aligned}
&M_j(t_0) = -D + \gamma R_0(\omega, t_0) + \gamma\alpha_n R_1(\omega, t_0) + O\left(\gamma\alpha_n^2\right),\\
&D \equiv \eta \int_{-\infty}^{\infty} \dot{x}_{h,j}^2(t)\,\mathrm{d}t > 0,\\
&R_0(\omega, t_0) \equiv \int_{-\infty}^{\infty} \dot{x}_{h,j}(t) \sin[\omega(t + t_0)]\,\mathrm{d}t,\\
&R_1(\omega, t_0) \equiv \int_{-\infty}^{\infty} (t + t_0)^{n+1} \dot{x}_{h,j}(t) \cos[\omega(t + t_0)]\,\mathrm{d}t.
\end{aligned} \tag{2}$$

Note that the price of expanding the MF (cf equation (2)) to discuss the appearance of simple zeros for $\alpha_n > 0$, while they do not appear for $\alpha_n = 0$, is that the limit $\lim_{t_0\to\pm\infty,\alpha_n\to 0}\alpha_n R_1(\omega, t_0)$ is not defined in such an expansion. However, this does not alter the validity of the present results since the limiting case $\alpha_n = 0$ corresponds to the well-known case of a periodic excitation. For such a purely periodic excitation ($\alpha_n = 0$), it is assumed in the following that the system does not exhibit transient chaos for a given set of parameter values, i.e. the MF (2) has no simple zeros:

$$D > \gamma|\max_{t_0\in\mathbb{R}} R_0(\omega, t_0)| \equiv \gamma A_0(\omega), \tag{3}$$

where $A_0(\omega)$ represents a chaotic-threshold function whose generic behavior is shown in figure 1. Indeed, homoclinic chaos is not possible for sufficiently small ω since a purely harmonic excitation becomes a constant when $\omega \to 0$. (Note that this is no longer valid in the absence of dissipation. The limiting Hamiltonian case will be considered elsewhere.) For sufficiently high ω, the dynamics can be analyzed using the vibrational mechanics approach [13] by separating $x(t) = z(t) + \psi(t)$, where $z(t)$ represents the slow dynamics while $\psi(t)$ is the fast oscillating term: $\psi(t) = \psi_0\cos(\omega t + \varphi_0)$ with $\psi_0 = \gamma\sqrt{\eta^2+\omega^2}/(\omega\eta^2 - \omega^3)$, $\varphi_0 = \arctan(\eta/\omega)$. On averaging out $\psi(t)$ over time, the slow reduced dynamics of the system becomes

$$\begin{aligned} &\ddot{z} + \mathrm{d}V/\mathrm{d}z = -\eta\dot{z}, \\ &\mathrm{d}V/\mathrm{d}z \equiv T^{-1}\int_0^T g[z + \psi_0\cos(\omega t + \varphi_0)]\,\mathrm{d}t, \end{aligned} \tag{4}$$

where $g(x) \equiv \mathrm{d}U(x)/\mathrm{d}x$, $T \equiv 2\pi/\omega$, i.e. that of a *purely* damped system, and hence homoclinic chaos is not possible when $\omega \to \infty$. Note that this demonstrates that equilibria are the *only* attractors of the system for $\alpha_n > 0$. Thus, one concludes that the properties $A_0(\omega \to 0, \infty) = 0$, $A_0(\omega) \geqslant 0$ imply via the extreme value theorem (Weierstrass' theorem [14]) that the generic chaotic threshold function $A_0(\omega)$ presents at least one maximum (the case shown in the inset of figure 1). Physically, the above scenario can be understood by considering the work done by a purely periodic temporal force: transient chaos is expected to appear for not too small energy transfer corresponding to a certain range of intermediate frequencies, but not in the limiting cases of very small and very large frequencies where the transfer of energy is insufficient to excite homoclinic events. Equation (2) indicates that the MF $M_j(t_0)$ has simple zeros (at sufficiently large values of t_0) for any positive value of the sweep rate because of the factor $(t + t_0)^{n+1}$ appearing in the definition of $R_1(\omega, t_0)$. Thus, this means that after a sufficiently long time, t_i, which depends upon the system's parameters and initial conditions, the instantaneous frequency of the autoresonant excitation reaches a threshold value $\Omega(t_i) = \omega_{\mathrm{th},1}$ that is the lowest frequency satisfying the relationship $D/\gamma = A_0(\omega_{\mathrm{th},1})$ (see figure 1, inset), i.e. the threshold condition for the onset of chaotic behavior. It is worth noting that this occurs for any initial condition because of the AR-induced increase of the system's energy. Thus, the condition $\Omega(t_i) = \omega_{\mathrm{th},1}$ implies the scaling law

$$t_i \sim (\omega_{\mathrm{th},1} - \omega)^{1/n}\alpha_n^{-1/n}, \tag{5}$$

for the onset time of transient chaos. Similarly, the lifetime τ of the chaotic transients can be estimated from the instantaneous frequency $\Omega(t_i + \tau) = \omega_{\mathrm{th},2}$ that is the lowest frequency satisfying the relationships $D/\gamma = A_0(\omega_{\mathrm{th},2})$, $\omega_{\mathrm{th},2} > \omega_{\mathrm{th},1}$ (see figure 1, inset), i.e.

$$\tau \sim [(\omega_{\mathrm{th},2} - \omega)^{1/n} - (\omega_{\mathrm{th},1} - \omega)^{1/n}]\alpha_n^{-1/n}. \tag{6}$$

We see that the general scaling laws (5) and (6) are *inverse-power* laws containing the two parameters (ω, α_n) that control the autoresonant excitation while the critical exponent is the inverse of the chirp order n. Notably, these scaling laws also contain the dependence upon the

particular potential, initial potential well, and dissipation and excitation strengths through the threshold frequencies $\omega_{\mathrm{th},1}$, $\omega_{\mathrm{th},2}$. Since the mid-1980s, critical exponents of chaotic transients have been discussed theoretically in the context of crises in dissipative maps [15]. The present theory establishes that an inverse-power law remains valid also for dissipative multistable flows subjected to autoresonant excitations. The connection between such results for maps and the present ones can be readily understood by assuming that for a purely periodic excitation ($\alpha_n = 0$) there exists a strange attractor for a certain frequency ($\omega_{\mathrm{th},1} < \omega < \omega_{\mathrm{th},2}$) instead of a periodic attractor ($\omega_{\mathrm{th},1} > \omega$) (see figure 1, inset). According to the above discussion, the strange attractor disappears for $\alpha_n > 0$ via a boundary crisis and chaotic transients appear instead, with $\alpha = \alpha_{n,c} \equiv 0$ being the critical value for the crisis. Therefore, since the non-existence of simple zeros of the MF is a sufficient condition for the disappearance of transient chaos, the lifetime of these chaotic transients follows the general inverse-power law

$$\tau \sim (\omega_{\mathrm{th},2} - \omega)^{1/n} \alpha_n^{-1/n}. \tag{7}$$

Now, applying EBAR theory one can deduce scaling laws relating both the onset time and lifetime to the autoresonant excitation amplitude. In particular, for Duffing-like potentials one has that the optimal amplitude scales as $\gamma \sim [3^n (n+1)!]^{3/(2n+2)} \alpha_n^{3/(2n+2)}$ [10] and hence the scaling law (7), for example, becomes $\tau \sim [(\omega_{\mathrm{th},2} - \omega)(n+1)!]^{1/n} \gamma^{-(2n+2)/(3n)}$, where one sees that the critical exponent ranges from $4/3$ for a linear chirp to $2/3$ for the highest order chirps.

From an experimental standpoint, it is also useful to discuss the lifetime of the corresponding metastable states in the initial and final potential wells. According to the above discussion, the lifetime of the states in the final potential well is infinite since these states are equilibria. Since it is assumed that the onset time of transient chaos occurs when the particle's energy reaches the energy level of the unperturbed separatrix for the first time, equation (5) also provides an estimate of the lifetime of the particle in the initial potential well for the case of AR excitations given by equation (1).

Numerical experiments confirmed the accuracy of the above scaling laws in different systems. Representative results corresponding to a dimensionless Duffing oscillator

$$\ddot{x} = x - x^3 - \eta \dot{x} + \gamma \,\mathrm{sn}[2K(m)\Omega(t)t/\pi; m] + \xi(t) \tag{8}$$

are shown in figures 2–5 for illustrative purposes. Here, $\mathrm{sn}(\cdot; m)$ is the Jacobian elliptic function of the parameter $m \in [0, 1]$ with $K(m)$ being the complete elliptic integral of the first kind. One has $\mathrm{sn}(\cdot; m = 0) = \sin(\cdot)$ while, in the other limit, $\mathrm{sn}(\cdot; m = 1)$ is the square-wave function. Note that, with the *instantaneous* period constant, solely the excitation shape is varied by increasing m from 0 to 1, and there is thus a smooth transition from a sine function to a square wave. Also, $\xi(t)$ is the (stationary Gaussian) fluctuating force associated with the coupling to the thermal bath. The fluctuation dissipation theorem [16] relates η and $\xi(t)$: $\langle \xi(t)\xi(t') \rangle = 2\eta\sigma\delta(t - t')$, where the normalized temperature σ controls the noise strength and $\delta(t - t')$ is the Dirac delta function. Numerically, the lifetime of transient chaos is defined by $\tau = t_f - t_i$, where t_i, t_f are the first and last instants, respectively, at which the particle's energy reaches the energy level of the unperturbed separatrix. In the presence of noise ($\sigma > 0$), an average over a number of realizations of equation (8) is taken to obtain the mean lifetime. For the purely deterministic ($\sigma = 0$) case of a sinusoidal ($m = 0$) excitation with a linear chirp ($n = 1$), for example, and after calculating the resulting integrals by residues, one obtains the corresponding MF:

$$\begin{aligned} M^{\pm}_{\mathrm{Duff}}(t_0) = &-D \mp B_0 \cos(\omega t_0) \pm \alpha_1 \left(B_2 + B_0 t_0^2\right) \sin(\omega t_0) \\ &\mp \alpha_1 B_1 t_0 \cos(\omega t_0) + O\left(\gamma \alpha_1^2\right), \end{aligned} \tag{9}$$

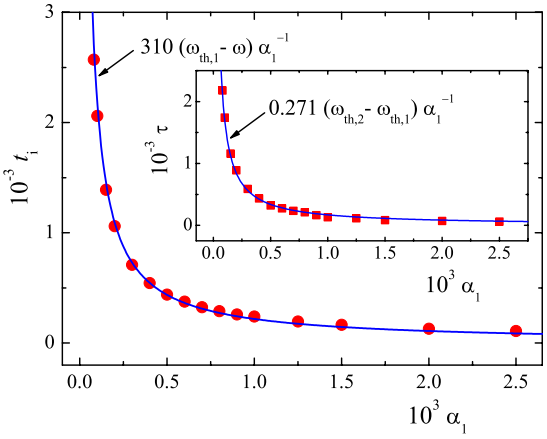

Figure 2. Onset time (circles), t_i, and lifetime (squares, inset), τ, of transient chaos corresponding to a dimensionless Duffing oscillator (equation (8)) for $m = 0, \sigma = 0, \eta = 0.5, \gamma = 0.4$ and $\omega = 0.493$. Hence, $\omega_{\mathrm{th},2} = 1.11736$, $\omega_{\mathrm{th},1} = 0.49371$ from $M^{\pm}_{\mathrm{Duff}}(t_0)$ (equation (9)). The solid lines indicate fits according to the scaling laws (5) and (6), respectively.

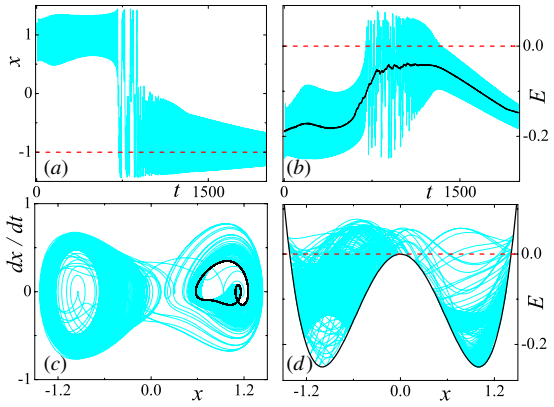

Figure 3. Autoresonant response of a dimensionless Duffing oscillator for a linear chirp $\alpha_1 = 3 \times 10^{-4}$ (equation (8)). (*a*) Position versus time and final equilibrium (dashed line). (*b*) Energy and average energy (over a few periods $2\pi/\omega$, thick black line) versus time. (*c*) Phase space trajectory and period-1 attractor existing at $\alpha_n = 0$ (thick black line). (*d*) Energy versus position (the dashed line indicates the separatrix energy level as in version (*b*)). The remaining parameters are the same as in figure 2.

where the sign +(−) corresponds to the right (left) homoclinic orbit of the unperturbed Duffing oscillator ($\eta = \gamma = 0$), and

$$D \equiv 4\eta/3,$$

$$B_0 \equiv \sqrt{2}\pi\gamma\omega \operatorname{sech}\left(\frac{\pi\omega}{2}\right),$$

$$B_1 \equiv 4\sqrt{2}\gamma\left[\frac{\pi}{2} - \frac{\pi^2\omega}{4}\tanh\left(\frac{\pi\omega}{2}\right)\right]\operatorname{sech}\left(\frac{\pi\omega}{2}\right),$$

$$B_2 \equiv \frac{\sqrt{2}}{8}\gamma\pi^2\operatorname{sech}^3\left(\frac{\pi\omega}{2}\right)[4\sinh(\pi\omega) - \pi\omega\cosh(\pi\omega) + 3\pi\omega].$$

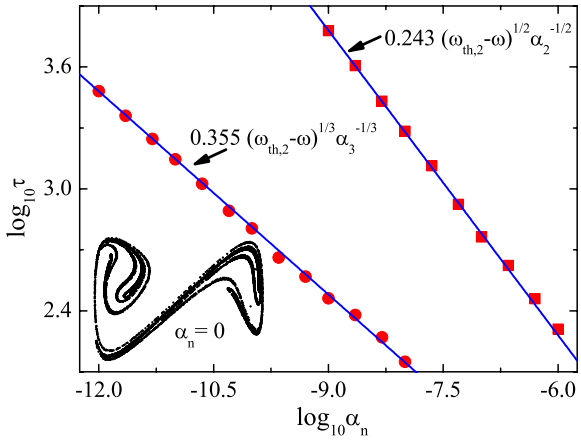

Figure 4. Lifetime of transient chaos corresponding to a dimensionless Duffing oscillator (equation (8)) for quadratic ($n = 2$, squares) and cubic ($n = 3$, circles) chirps. The solid lines indicate fits according to the scaling law (7). Also shown is the strange attractor existing at $\alpha_{2,3} = 0$. Fixed parameters: $m = 0, \sigma = 0, \eta = 0.154, \gamma = 0.2, \omega = 1.1$. Hence, $\omega_{\mathrm{th},2} = 1.714\,04$ from $M^{\pm}_{\mathrm{Duff}}(t_0)$ (equation (9)).

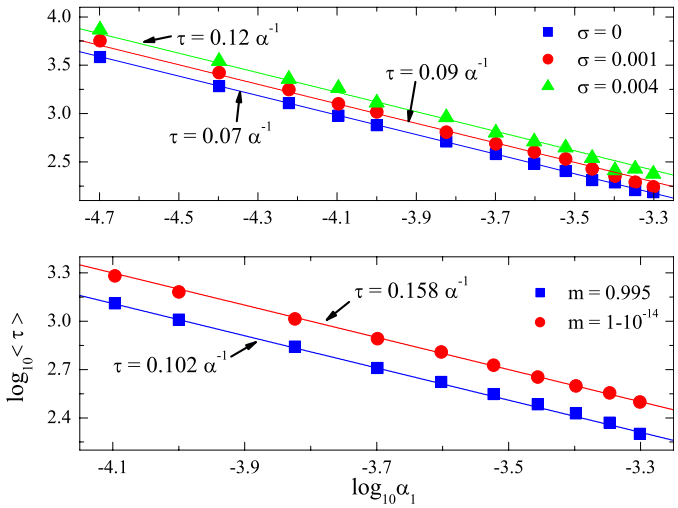

Figure 5. Mean lifetime of transient chaos corresponding to a dimensionless Duffing oscillator (equation (8)) for a linear chirp in the presence of noise (top panel, $m = 0, \gamma = 0.4$) and subjected to elliptic excitations (bottom panel, $\sigma = 0, \gamma = 0.3$). The solid lines indicate fits according to the scaling law (6). Fixed parameters: $\eta = 0.5, \omega = 0.493$.

The results for the case of a periodic (chaotic) attractor existing at $\alpha_n = 0$ are shown in figure 2 (figure 4). While a linear chirp is considered in figures 2 and 3, figure 4 shows the results for quadratic and cubic chirps. Figures 2 and 4 show excellent agreement between the numerical results and the predicted scaling laws for both the onset time and the lifetime of transient chaos. Figure 3(*b*) shows the AR-induced increase of energy over time until the separatrix energy level is reached, indicating the onset of transient chaos (see figures 3(*a*)

and (*d*)), followed by a decrease of energy when the dynamics becomes effectively purely dissipative (see figure 3(*c*)). Note that the average energy remains roughly constant during transient chaos. The robustness of the scaling laws versus both the presence of additive noise and re-shaping of the autoresonant excitation is shown in figure 5. Note that, for the elliptic excitation, $\omega_{\mathrm{th},i}$, $i = 1, 2$, are functions of m, which is the reason for the different prefactors in the fits for $m = 0.995$ and $m = 1 - 10^{-14}$ (figure 5, bottom). For the noisy case (figure 5, top), the origin of the different prefactors in the fits for $\sigma = 0$, $\sigma = 0.001$ and $\sigma = 0.004$ may be analyzed on the basis of a stochastic MA (the analysis is beyond the scope of the present work).

In summary, general inverse-power laws relating both the onset and lifetime of transient chaos and the parameters of escape-inducing autoresonant excitations have been theoretically derived for generic, dissipative and multistable flows. Numerical simulations showed the robustness of these scaling laws against both the presence of additive noise and driving re-shaping. Since the critical exponents were found to solely depend on the chirp's order, such scaling laws are expected to remain valid for even more general dissipative systems including spatiotemporal chaotic systems [17]. The present results can be readily tested experimentally (for example in mechanical and laser systems as well as in the areas of electrical engineering and environmental studies [18]) and can find an application to optimally control elementary dynamic processes characterized by chaotic escapes from a potential well, such as diverse atomic and molecular processes, transport phenomena in dissipative lattices and control of the electron dynamics in quantum solid-state devices. Regarding quantum systems, Josephson tunnel junctions are among the main candidates where the above scaling laws could be experimentally confirmed. In such a case, a classical description is given by the resistively and capacitively shunted junction model [19].

Acknowledgments

The author thanks Francisco Balibrea for stimulating discussions and Pedro J Martínez for help with the stochastic numerical code and stimulating discussions. The work is partially supported by the Spanish MCI through project FIS2008-01383.

References

[1] Grossmann F *et al* 1991 *Phys. Rev. Lett.* **67** 516
[2] Benzi R, Sutera A and Vulpiani A 1981 *J. Phys. A: Math. Gen.* **14** L453
Gammaitoni L *et al* 1998 *Rev. Mod. Phys.* **70** 223
[3] Holtaus M 1992 *Phys. Rev. Lett.* **69** 1596
[4] Pekola J P *et al* 2005 *Phys. Rev. Lett.* **95** 197004
[5] Kramers H A 1940 *Physica* **7** 284
[6] Krempl S *et al* 1992 *Phys. Rev. Lett.* **69** 430
[7] Fainberg B D, Jouravlev M and Nitzan A 2007 *Phys. Rev.* B **76** 245329
[8] Goswami D 2003 *Phys. Rep.* **374** 385
[9] Bohm D and Foldy L 1946 *Phys. Rev.* **70** 249
Malhotra R 1993 *Nature* **365** 819
Fajans J and Friedland L 2001 *Am. J. Phys.* **69** 1096
Liu W K, Wu B and Yuan J M 1995 *Phys. Rev. Lett.* **75** 1292
[10] Chacón R 2005 *Europhys. Lett.* **70** 56
Chacón R 2008 *Phys. Rev.* E **78** 066608
[11] Taki M 1987 *Phys. Rev.* B **35** 3267

[12] Melnikov V K 1963 *Tr. Mosk. Ova.* **12** 3
Melnikov V K 1963 *Trans. Moscow Math. Soc.* **12A** 1 (Engl. Transl.)
Guckenheimer J and Holmes P J 1983 *Nonlinear Oscillations, Dynamical Systems and Bifurcation of Vector Fields* (Berlin: Springer)
Lichtenberg A J and Lieberman M A 1983 *Regular and Stochastic Motion* (New York: Springer)
[13] Bleckman I I 2000 *Vibrational Mechanics* (Singapore: World Scientific)
[14] Keisler H J 1986 *Elementary Calculus. An Infinitesimal Approach* (Boston, MA: Weber & Schmidt)
[15] Grebogi C, Ott E and Yorke J A 1986 *Phys. Rev. Lett.* **57** 1284
Alligood K T, Sander E and Yorke J A 2006 *Phys. Rev. Lett.* **96** 244103 and references therein
[16] Risken H 1996 *The Fokker-Planck Equation: Methods of Solutions and Applications* (Berlin: Springer)
Greenside H S and Helfand E 1981 *Bell Syst. Tech. J.* **60** 1927
[17] Rempel E L and Chian A C-L 2007 *Phys. Rev. Lett.* **98** 014101
Peixinho J and Mullin T 2006 *Phys. Rev. Lett.* **96** 094501
[18] Dhamala M and Lai Y-C 1999 *Phys. Rev.* E **59** 1646 and references therein
[19] Barone A and Paternó G 1982 *Physics and Applications of the Josephson Effect* (New York: Wiley)